Electronic Supplementary Information

AIE active mechanochromic materials based N-phenylcarbazol-substituted tetraarylethene for OLED applications

He Zhao,[a] Yang Wang,[b] Yongtao Wang,*[a] Gufeng He,*[b] Mei Xue,[a] Pingan Guo,[a] Bin Dai,*[a] Zhiyong Liu[a] and Yu Qi [a]

[a] *School of Chemistry and Chemical Engineering/Key Laboratory for Green Processing of Chemical Engineering of Xinjiang Bingtuan, Xinjiang Shihezi University, Shihezi 832003, China.*
[b] *National Engineering Lab for TFT-LCD Materials and Technologies, and Department of Electronic Engineering, Shanghai Jiao Tong University, Shanghai 200240, China*

Table of Contens

illumination.

Fig. S10. (A) Emission spectra of MeNPCE in THF and THF/water mixtures with varying water fractions (f_w). (B) Emission intensity increase of MeNPCE in different aqueous mixtures. Concentration: 10 μM; excitation wavelength: 360 nm. Photographs in (B) are MeNPCE in THF and 10/90 THF-water mixture taken under 365 nm UV light illumination.

Fig. S11 TEM image of nanoaggregates of NPCE (A), MeNPCE (B) and MeONPCE (C) formed in THF/water mixtures with 90% water fractions.

Fig. S12. Absorption spectra of NPCE (A), MeNPCE (B) and MeONPCE (C) in THF and THF/water mixtures with varying water fractions (f_w).

Fig. S13. Emission maxima of MeONPCE during the grinding-fuming cycles. As = as prepared sample, G = ground sample; F= Fumed sample (fumed in DCM for 3 min). The numbers after G or F represent cycle numbers.

Fig. S14. TGA and DSC (inset) thermograms of NPCE (A) and MeNPCE (B) recorded under nitrogen atmosphere at the scan rates of 10 ^{o}C min^{-1}.

Fig. S15. Representative cyclic voltammogram of NPCE (A) and MeNPCE (B) measured in dry dichloromethane solution, containing 0.1 M $TBAPF_6$ at 25 ^{o}C.

Table S1. Electrochemical data for NPCE, MeNPCE and MeONPCE.

Fig. S16. (A) Amorphous PL spectra and (B) EL spectra of NPCE, MeNPCE and MeONPCE.

Fig. S17 CIE coordinates of the all OLED devices.

Experimental Section

Chemicals and instruments.

All the reagents were obtained from commercial sources and used without further purification. The organic solvents were of analytical grade quality and all were dried by traditional methods. In general, all the intermediates and final compounds were purified by column chromatography on silica gel (200-300 mesh), and crystallization from analytical grade solvents. Reactions were monitored by using thin layer chromatography (TLC) (Qingdao Jiyida silica gel reagent factory GF254).

^{1}H NMR (400 MHz) and ^{13}C NMR (100 MHz) spectra was obtained with a Varian inova instrument using tetramethylsilane (TMS) as the internal standard. ESI/MS spectra were obtained on a Waters GCT Premier. MALDI/LRMS (HRMS) was obtained on a UltrafleXtreme MALDI-TOF/TOF mass spectrometer (Bruker, Germany). UV-vis absorption and emission measurements were performed on a MaPada UV-3200PCS spectrophotometer and a Hitachi F-2500 fluorospectrometer, respectively. Emission quantum yields of the luminogens in solvents were estimated by using quinine sulfate as standard, while solid-state efficiencies were determined using a FLS920 Fluorescence Lifetime and Steady State Spectroscopy with the excitation wavelength of 365 nm. Glass transition temperature was determined by DSC measurements carried out using Netzsch Gerätebau GmbH R.O. Thermal stability was determined by thermogravimetric analyzer (TGA, Netzsch STA449F3) over a temperature range of 25-1000 ^{o}C at a heating rate of 10 ^{o}C min^{-1} under a nitrogen atmosphere. The electrochemical measurements were carried out with an EPSILON potentiostat (BAS). Cyclic voltammograms were recorded at scan rates of 50, 100, and 200 mV s^{-1} from a solution of NPCE, MeNPCE and MeONPCE (10^{-3} mol dm^{-3}) in dichloromethane solution containing 0.1 mol dm^{-3} tetrabutylammonium hexafluorophosphate ($TBAPF_6$), using a gastight single-compartment three-electrode cell equipped with carbon working, platinum wire auxiliary, and saturated calomel electrode pseudo-reference electrodes. Peak potential was determined versus ferrocene as internal standard. Powder XRD measurements were conducted on D8

Advance (Bruker) with Cu Kα radiation in the range $10^{o} < 2\theta < 90^{o}$. Digital photographs were taken by Canon 550D (Canon, Japan) digital cameras.

OLED fabrication.

The electroluminescence devices were fabricated by following processes. First, ITO-coated glass substrates were cleaned sequential using deionized water, acetone and isopropanol in an ultrasonic bath, and then dried in drying cabinet followed by pretreatment with oxygen plasma. Then the organic films of 1,4-bis[(1-naphthylphenyl)-amino]biphenyl, NPCE, MeNPCE, MeONPCE, 2,2',2''-(1,3,5-benzinetriyl)tris(1-phenyl-1-H-benzimidazole) (TPBI), were deposited by the thermal evaporation under a base vacuum of about 10^{-6} torr. Finally, the samples were then transferred to the metal chamber for cathode deposition which composed of 1 nm LiF capped with 100 nm Al. Al metal was evaporated in another vacuum chamber without breaking the vacuum. The thicknesses of the films were determined by quartz thickness monitors. The active area of the EL device, defined by the overlap of the ITO and the cathode electrode, was 3 mm × 3 mm. Current density-voltage (J-V) and current efficiency-current density (CE-J) characteristics were measured with a computer controlled Keithley 2400 Source Meter and BM-7A Luminance Colorimeter. The electroluminescence spectra were measured by Labsphere CDS-610. All measurements were carried out under air at room temperature without device encapsulation.

Synthesis

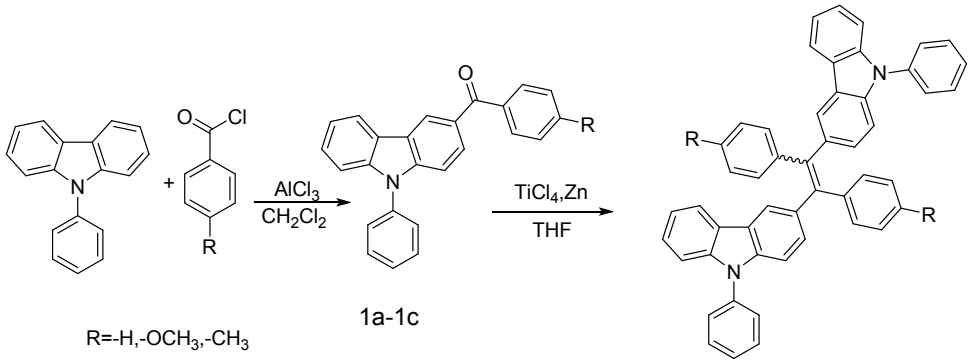

Scheme S1. Synthetic routes to NPCE, MeNPCE and MeONPCE.

Synthesis of N-phenyl-3-benzoylcarbazole[1] (1a): The 3 g (12.34 mmol) of N-phenylcarbazole was dissolved in 10 mL anhydrous dichloromethane solution. Then 1.953 g (14.81 mmol) of $AlCl_3$ was quickly added in the stirred mixture solution. When the temperature reached 0 ^oC, 1.71 mL (14.81 mmol) benzoylchloride solution was slowly added dropwise to the stirred mixture solution under nitrogen. After the addition the mixture was stirred at room temperature for 2 h. The reaction was quenched by addition of ice water and extraction with CH_2Cl_2 (3×50 mL). The combined ethereal extracted was dried over anhydrous Na_2SO_4 and evaporated to dryness to leave a light yellow residue, The crude product was recrystallized from ethyl acetate to give white acicular crystal (yield 85%): m.p. 172.1-172.3 ^oC. ^1H NMR (DMSO-d_6, 400 MHz): (ppm) 8.69 (s, 1H), 8.34 (d, 1H, J = 7.6 Hz), 7.84 (dd, 1H, J_1 = 8.8 Hz, J_2 = 0.8 Hz), 7.76 (d, 2H, J = 7.6 Hz), 7.67 (m, 5H), 7.56 (t, 3H, J = 7.6 Hz), 7.46 (m, 2H), 7.34 (m, 2H). LC-MS (ESI): m/z 348.3 $[M+H]^+$.

Synthesis of N-phenyl-3-(4-methyl)benzoylcarbazole (1b)**:** The Synthetic procedure of 1b is similar to that of 1a described above. Yield : 86%; white crystals; m.p. 148.7-149.0 ^oC; ^1H NMR (DMSO-d_6, 400 MHz): (ppm) 8.66 (s, 1H), 8.34 (d, 1H, J = 7.6 Hz), 7.82 (dd, 1H, J_1 = 8.4 Hz, J_2 = 1.2 Hz), 7.63 (m, 7H), 7.39 (m, 6H), 2.41 (s, 3H). MALDI-TOF MS: m/z 384.1 $[M + Na]^+$.

Synthesis of N-phenyl-3-(4-methoxyl)benzoylcarbazole (1c): The Synthetic procedure of 1c is similar to that of 1a described above. Yield : 89%; white crystals; m.p. 147.8-148.1 oC; 1H NMR (DMSO-d_6, 400 MHz): (ppm) 8.67 (d, 1H, J = 1.6 Hz), 8.36 (d, 1H, J = 7.6 Hz), 7.81 (m, 3H), 7.64 (m, 5H), 7.42 (m, 4H), 7.10 (dd, 2H, J_1 = 11.6 Hz, J_2 = 2.8 Hz), 3.87 (s, 3H). LC-MS (ESI): m/z 378.1 $[M+H]^+$.

Synthesis of 1,2-diphenyl-1,2-bis(9-phenyl-9H-carbazol-3-yl)ethene[2, 3] (NPCE)**:** In a two-necked flask equipped with a magnetic stirrer and a reflux condenser were added 0.21 g (3.2 mmol) of zinc powder and 0.50 g (1.34 mmol) of N-phenyl-3-benzoylcarbazole. The flask was evacuated under vacuum and flushed with dry nitrogen three times. 10 mL of THF was then added. The mixture was cooled to −78 °C and $TiCl_4$ (0.44 mL, 4 mmol) was slowly added dropwise by a syringe at under nitrogen. The mixture was slowly warmed to room temperature. After stirred for 0.5

h, the mixture was refluxed for 24 h. After cooled to room temperature, the reaction was quenched with 10% K_2CO_3 aqueous solution and filtered. The filtrate was extracted with $CHCl_3$. The organic layer was washed with water and dried over Na_2SO_4. The crude product was purified by silica-gel chromatography [petroleum ether (PE): dichloromethane (DCM) = 10:3] to give a yellow solid in 85% yield. ^{1}H NMR ($CDCl_3$, 400 MHz): (ppm) 7.96-7.78 (m, 4H), 7.60-7.46 (m, 8H), 7.46-7.35 (m, 4H), 7.35-7.37 (m, 3H), 7.22-7.19 (m, 1H), 7.19-7.13 (m, 8H), 7.13-7.08 (m, 3H), 7.08-7.02 (m, 3H). ^{13}C NMR (DMSO-d_6, 100 MHz): (ppm) 144.894, 144.86, 141.00, 140.95, 140.77, 140.75, 139.40, 139.33, 137.68, 137.63, 136.29, 136.23, 131.69, 131.65, 130.16, 130.03, 129.75, 129.68, 127.63, 127.58, 127.25, 127.17, 126.92, 126.88, 126.13, 126.09, 125.69, 125.61, 123.48, 123.47, 123.31, 123.26, 122.98, 122.94, 120.34, 120.2, 119.81, 119.73, 109.73, 109.67, 108.93, 108.83. LC-MS (ESI): m/z 663.2 $[M+H]^+$, HRMS (MALDI-TOF): m/z 662.2713 $[(M)^+$, calcd 662.2716].

Synthesis of 1,2-bis(9-phenyl-9H-carbazol-3-yl)-1,2-di-p-tolylethene (MeNPCE): The Synthetic procedure of MeNPCE is similar to that of NPCE described above, a yellow solid was obtained in 80% yield. ^{1}H NMR ($CDCl_3$, 400 MHz): (ppm) 8.02-7.85 (m, 4H), 7.64-7.30 (m, 16H), 7.28-7.04 (m, 8H), 6.99 (d, 2H, J = 8 Hz), 6.91 (d, 2H, J = 8 Hz), 2.43-2.19 s, 6H, -CH_3). ^{13}C NMR ($CDCl_3$, 100 MHz): (ppm) 142.12, 142.06, 141.02, 140.97, 140.26, 139.38, 139.28, 137.79, 137.71, 136.78, 135.62, 135.53, 131.62, 131.53, 130.31, 130.14, 129.78, 129.69, 128.39, 127.24, 127.15, 126.95, 126.90, 125.66, 125.58, 123.64, 123.57, 123.32, 123.01, 120.40, 119.81, 119.73, 109.75, 109.68, 108.90, 21.30, 21.24. LC-MS (MALDI-TOF): m/z 690.3 $[M]^+$, HRMS (MALDI-TOF): m/z 690.3037 $[(M)^+$, calcd 690.3030].

Synthesis of 1,2-bis(4-methoxyphenyl)-1,2-bis(9-phenyl-9H-carbazol-3-yl)ethene (MeONPCE):The Synthetic procedure of MeONPCE is similar to that of NPCE described above, a white solid was obtained in 70% yield. ^{1}H NMR ($CDCl_3$, 400 MHz): (ppm) 8.00-7.72 (m, 3H), 7.59-7.28(m, 16H), 7.22-7.01 (m, 9H), 6.75-6.52 (m, 4H), 3.85-3.61 (s, 6H, -OCH_3). ^{13}C NMR ($CDCl_3$, 100 MHz): (ppm) 157.72, 140.96, 139.316, 137.68, 136.82, 136.74, 132.82, 130.29, 130.16, 129.74, 129.64, 127.21, 127.11, 126.91, 126.86, 125.63, 125.53, 123.51, 123.49, 123.22, 122.93, 120.31,

119.77, 119.68, 112.99, 109.71, 109.63, 108.83, 55.09, 55.01. LC-MS (ESI): m/z 723.2 $[M+H]^+$, HRMS (MALDI-TOF): m/z 722.2929 $[(M)^+$, calcd 722.2928].

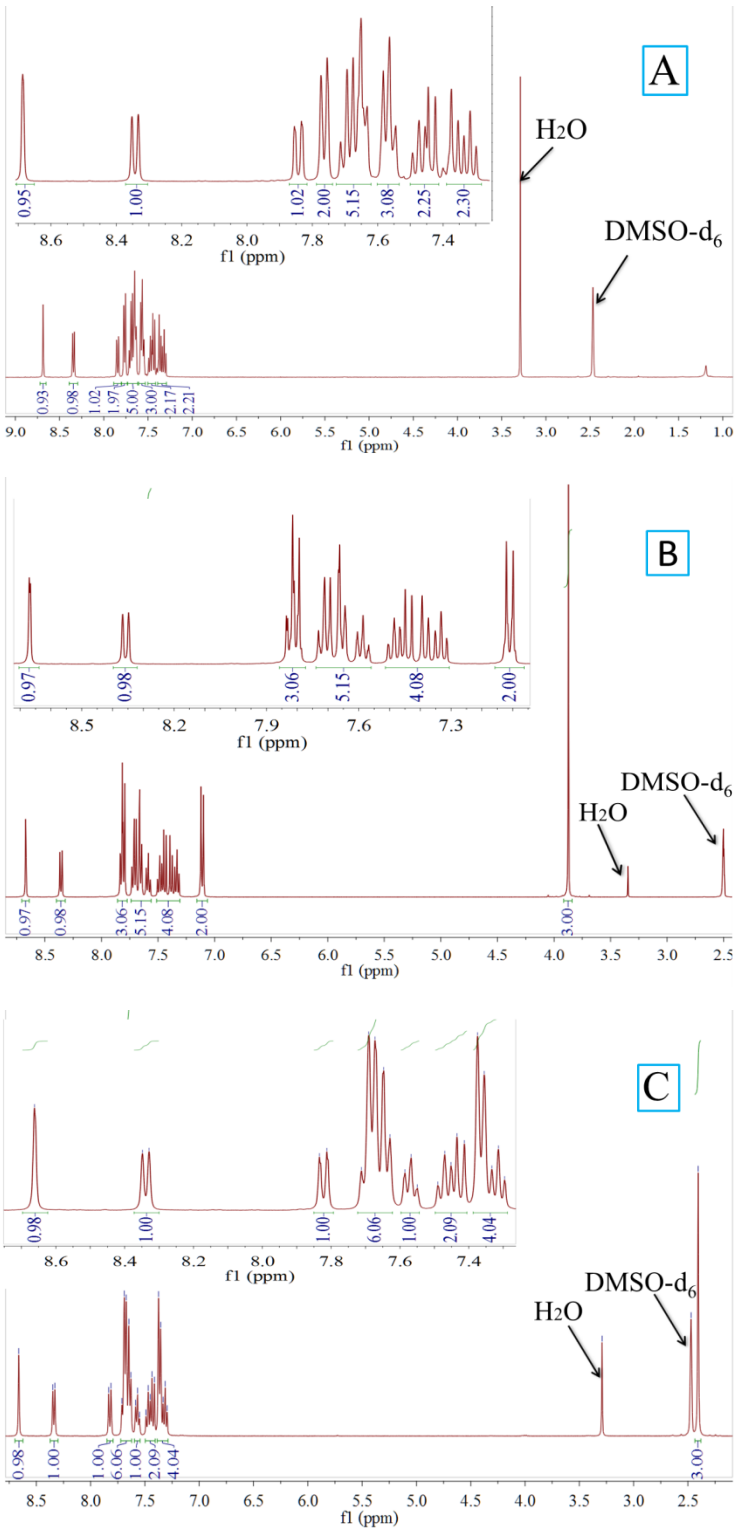

Fig. S1 ^{1}H NMR spectra of 1a (A), 1b (B) and 1c(C).

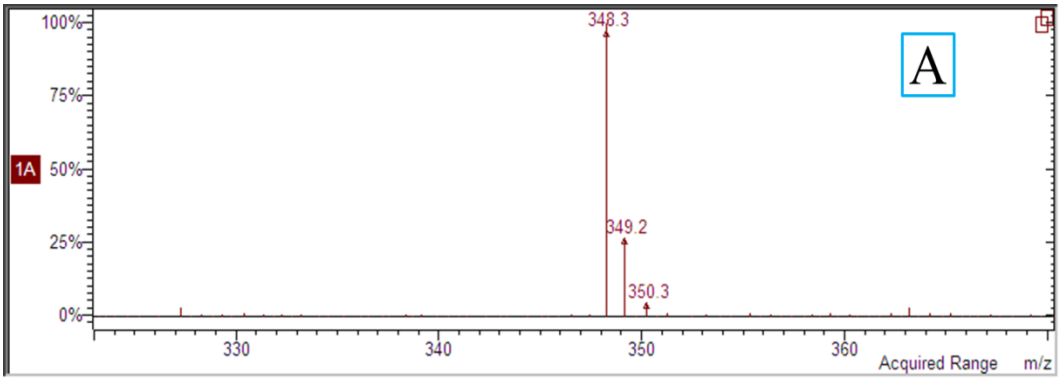

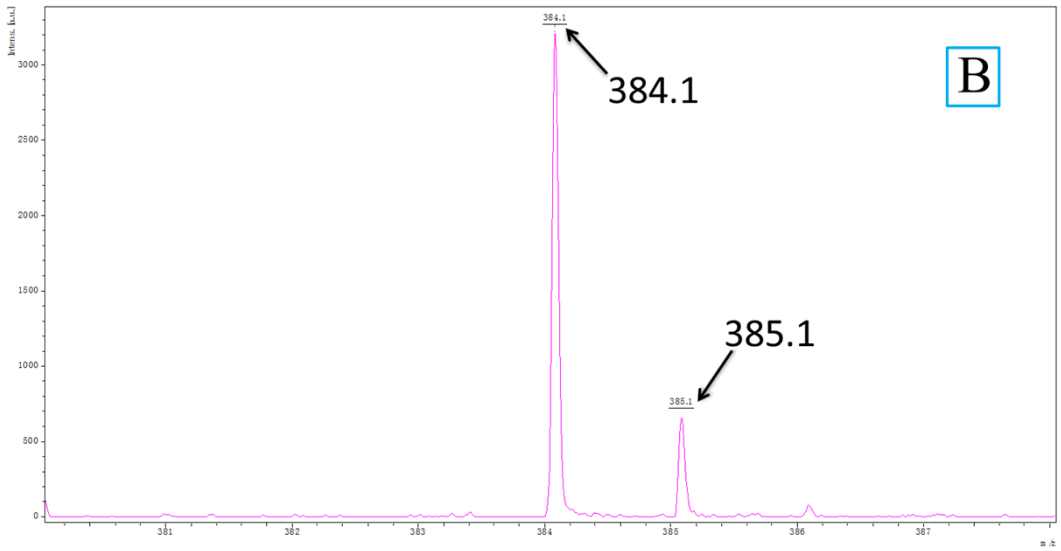

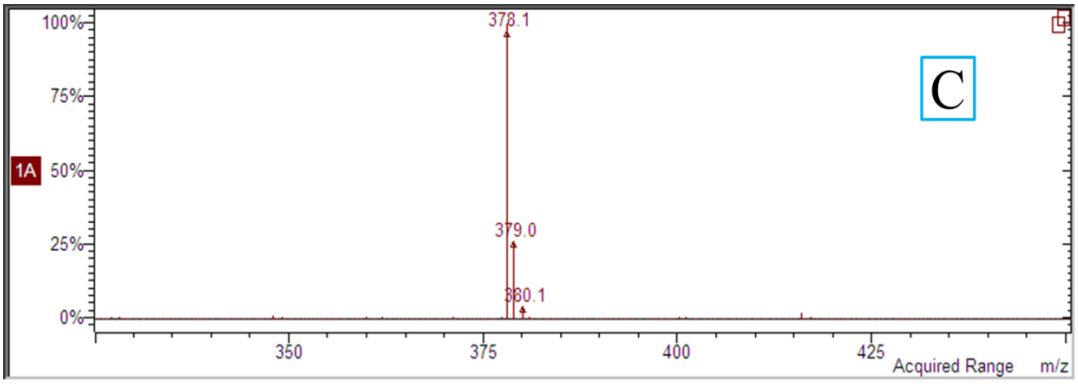

Fig. S2 LRMS spectra of 1a (A), 1b (B) and 1c(C).

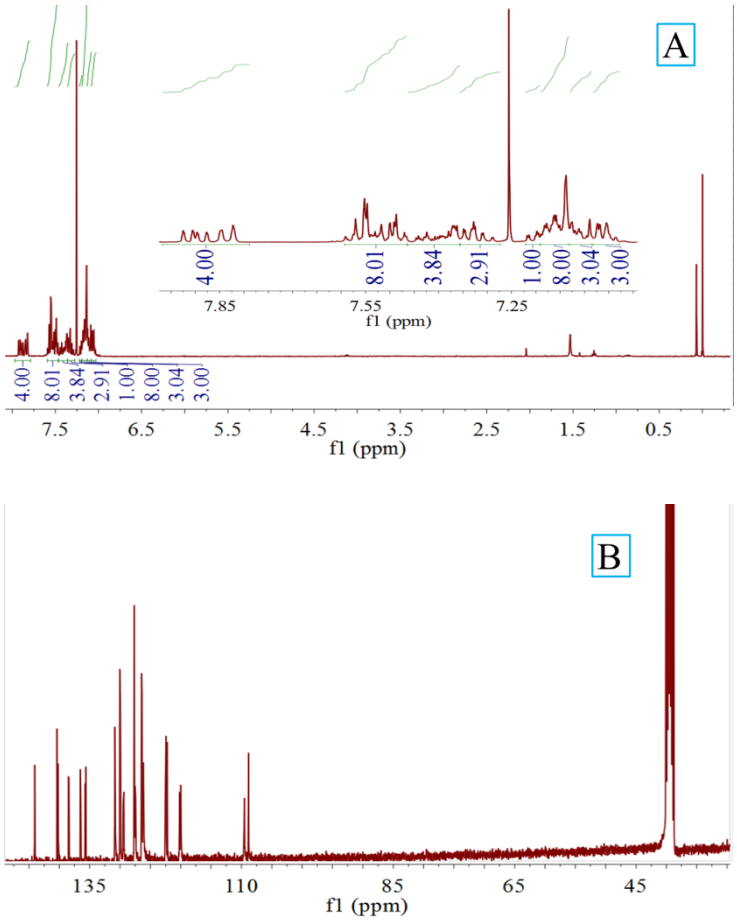

Fig. S3 (A) ^{1}H NMR and (B) ^{13}C NMR spectra of NPCE.

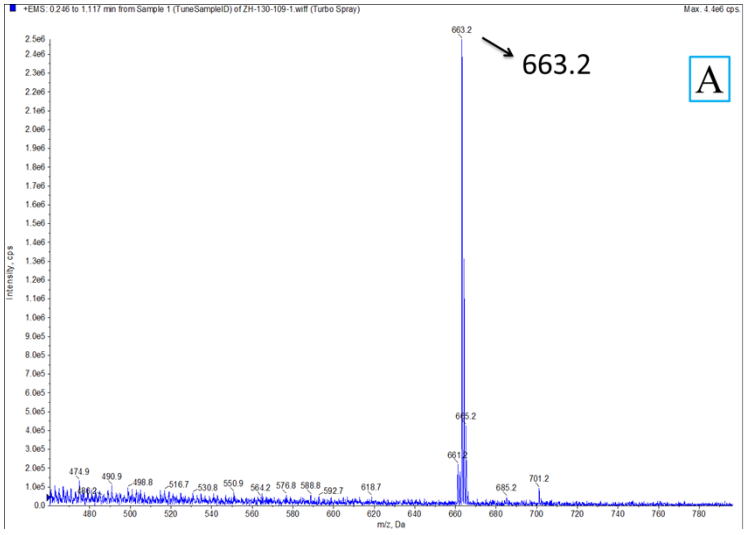

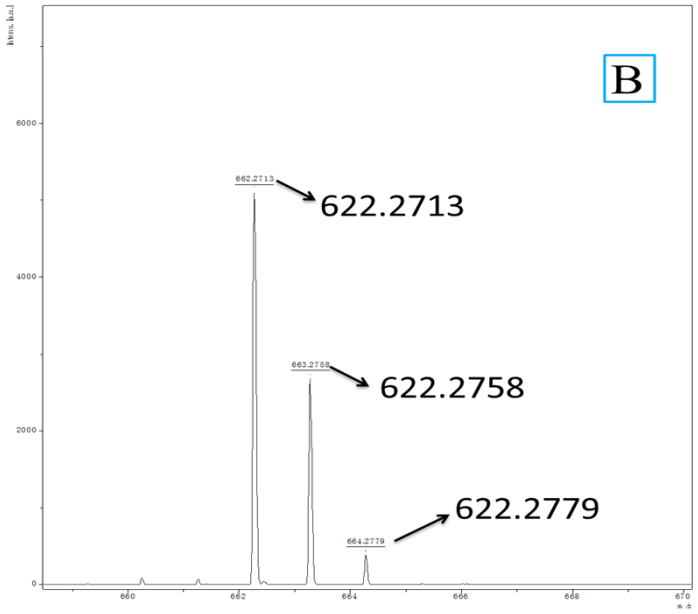

Fig. S4 (A) LRMS and (B) HRMS spectra of NPCE.

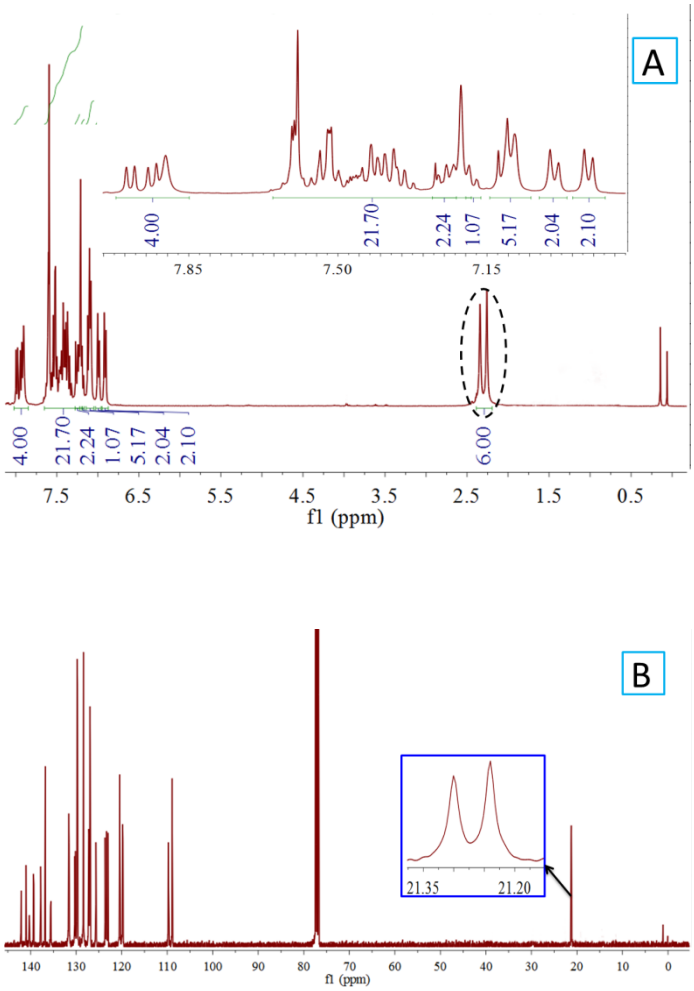

Fig. S5 (A) ^{1}H NMR and (B) ^{13}C NMR spectra of MeNPCE.

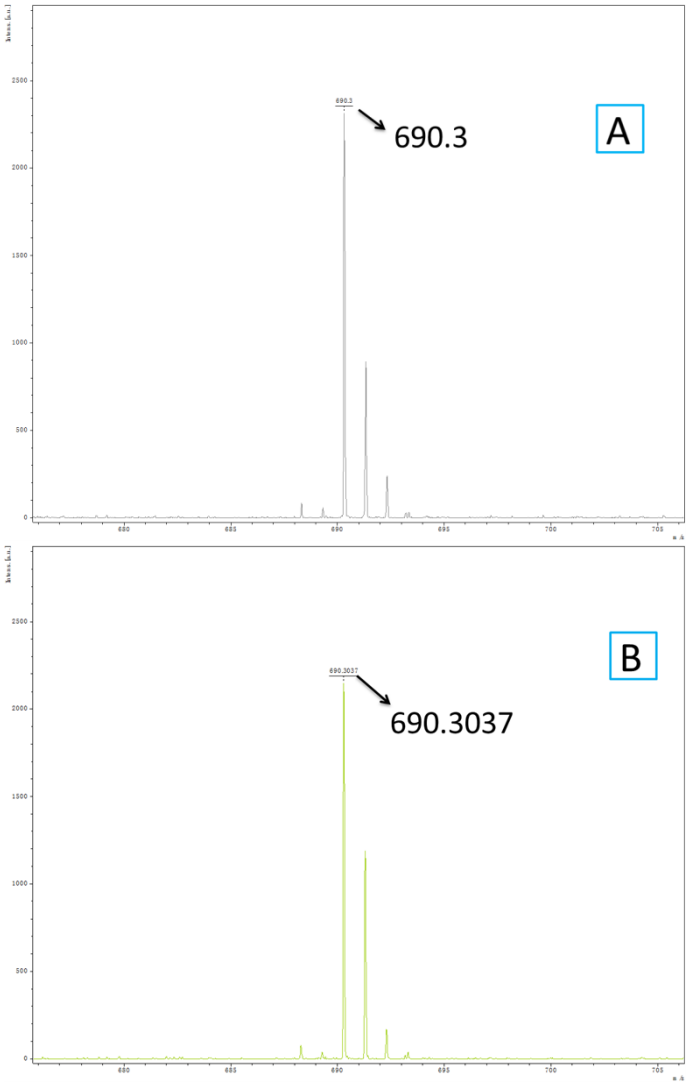

Fig. S6 (A) LRMS and (B) HRMS spectra of MeNPCE.

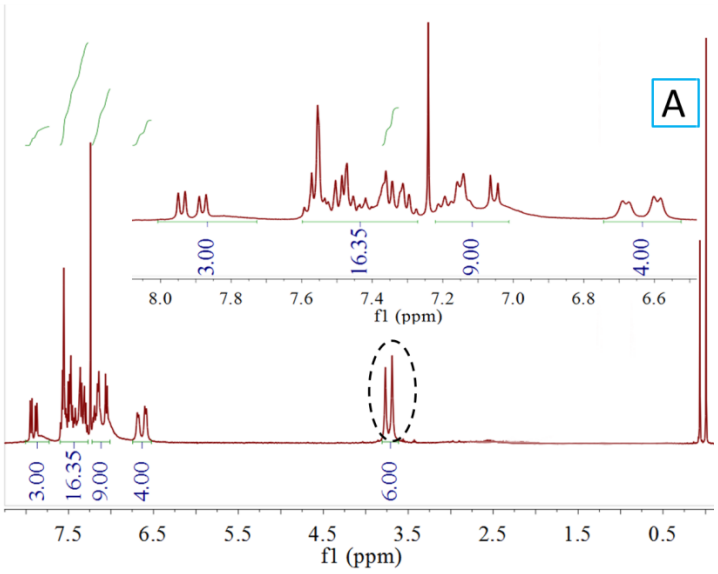

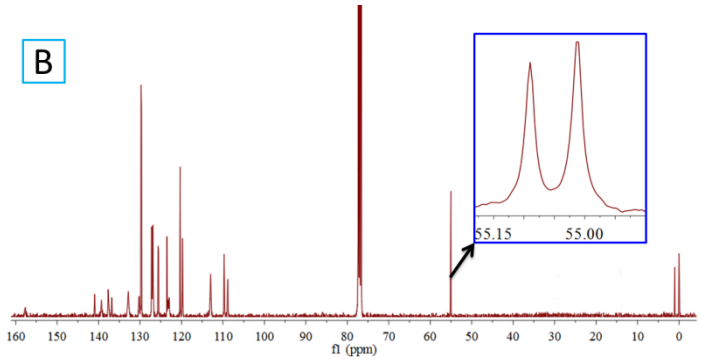

Fig. S7 (A) ^{1}H NMR and (B) ^{13}C NMR spectra of MeONPCE.

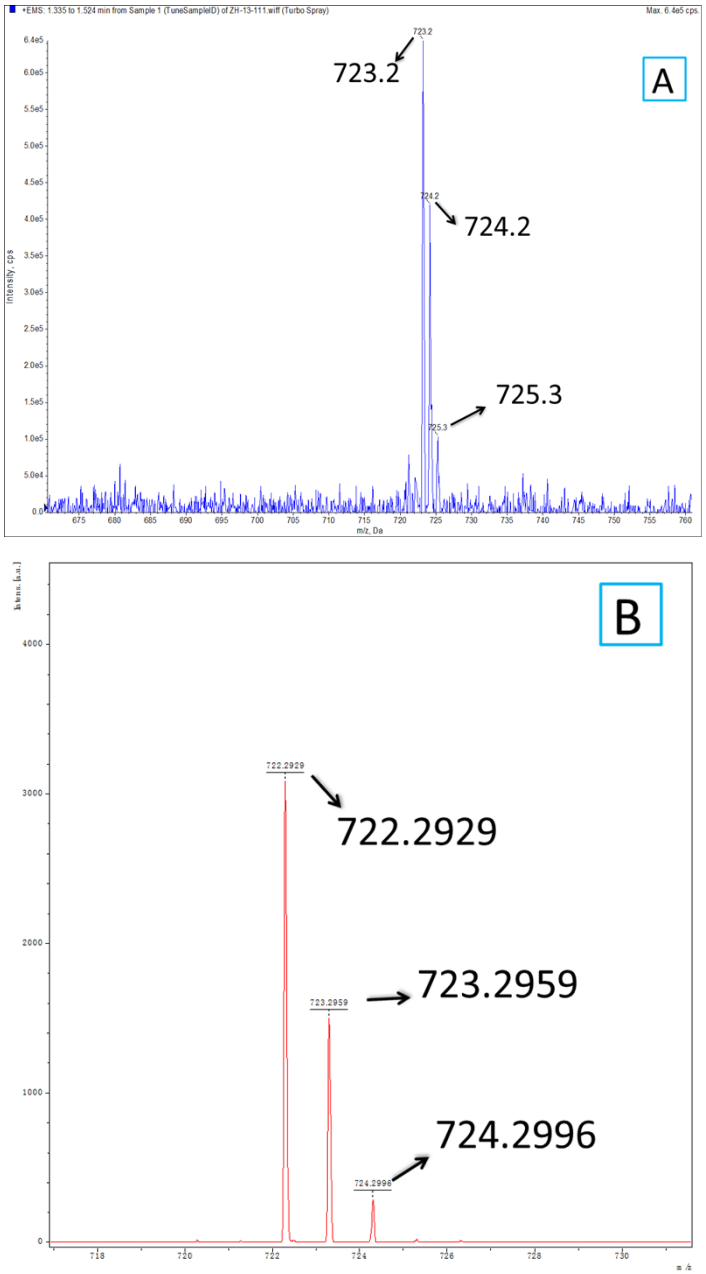

Fig. S8 (A) LRMS and (B) HRMS spectra of MeONPCE.

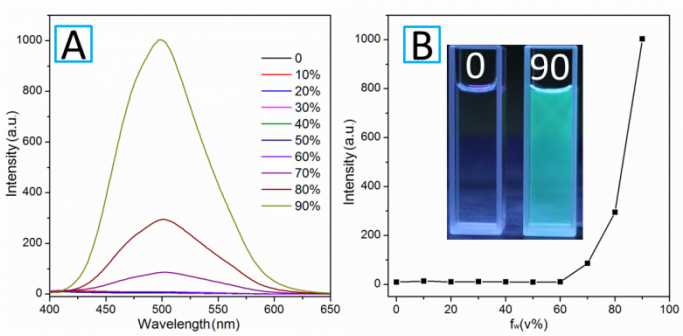

Fig. S9 (A) Emission spectra of NPCE in THF and THF/water mixtures with varying water fractions (f_w). (B) Emission intensity increase of NPCE in different aqueous mixtures. Concentration: 10 μM; excitation wavelength: 360 nm. Photographs in (B) are NPCE in THF and 10/90 THF-water mixture taken under 365 nm UV light illumination.

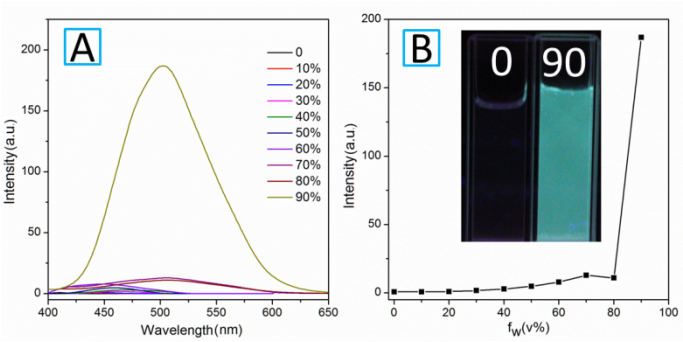

Fig. S10 (A) Emission spectra of MeNPCE in THF and THF/water mixtures with varying water fractions (f_w). (B) Emission intensity increase of MeNPCE in different aqueous mixtures. Concentration: 10 μM; excitation wavelength: 360 nm. Photographs in (B) are MeNPCE in THF and 10/90 THF-water mixture taken under 365 nm UV light illumination.

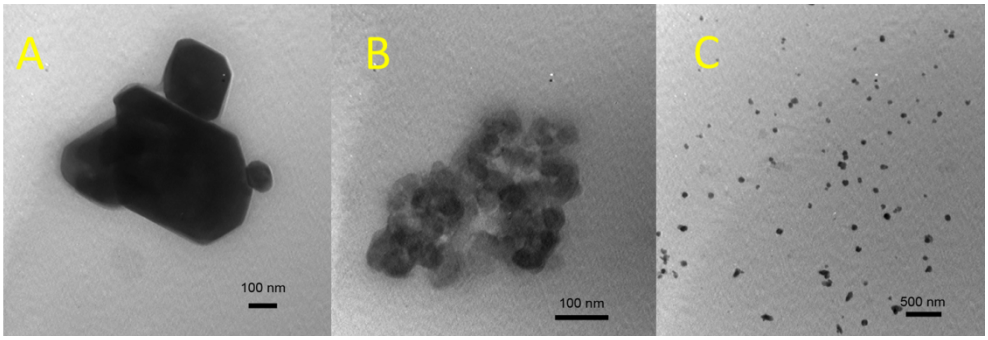

Fig. S11 TEM image of nanoaggregates of NPCE (A), MeNPCE (B) and MeONPCE (C) formed in THF/water mixtures with 90% water fractions.

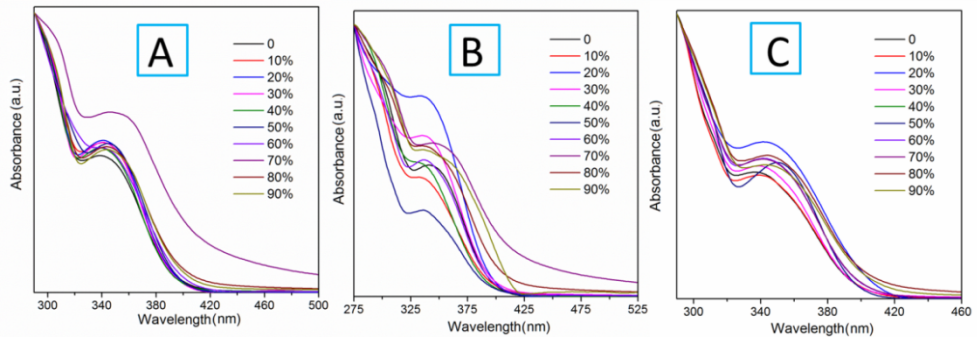

Fig. S12 Absorption spectra of NPCE (A), MeNPCE (B) and MeONPCE (C) in THF and THF/water mixtures with varying water fractions (f_w).

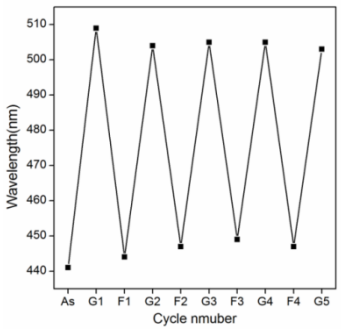

Fig. S13 Emission maxima of MeONPCE during the grinding-fuming cycles. As = as prepared sample, G = ground sample; F= Fumed sample (fumed in DCM for 3 min). The numbers after G or F represent cycle numbers.

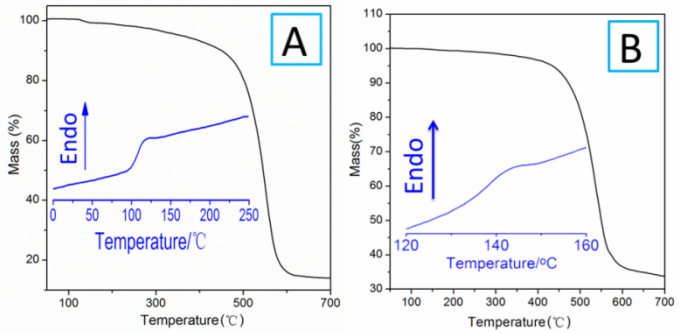

Fig. S14 TGA and DSC (inset) thermograms of NPCE (A) and MeNPCE (B) recorded under nitrogen atmosphere at the scan rates of 10 °C min^{-1}.

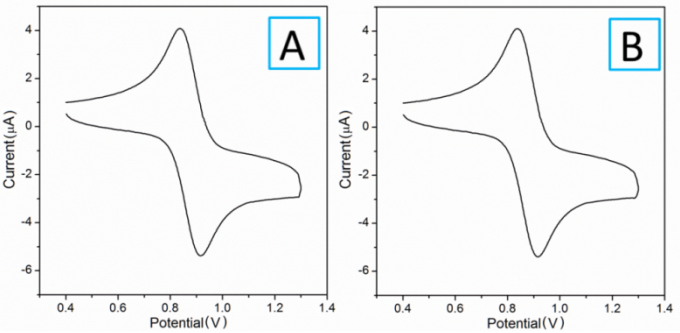

Fig. S15 Representative cyclic voltammogram of NPCE (A) and MeNPCE (B) measured in dry dichloromethane solution, containing 0.1 M $TBAPF_6$ at 25 °C.

Table 1 Electrochemical data for NPCE, MeNPCE and MeONPCE.[a]

Compound	$E_{onset\text{-}ox}$ (V)	E_{HOMO} (eV)	E_{LUMO} (eV)	E_g (eV)
NPCE	0.91	-5.31	-1.94	3.37
MeNPCE	0.91	-5.31	-1.95	3.36
MeONPCE	0.80	-5.20	-1.86	3.34

[a] Abbreviation: $E_{onset\text{-}ox}$ = onset oxidation potential measured by cyclic voltammetry, HOMO = highest occupied molecular orbital derived by the equation: HOMO = ($E_{onset\text{-}ox}$+4.8−$E_{ferrocene}$) eV, where the value of $E_{ferrocene}$ measured in our experiment was 0.4 eV, E_g= energy band gap, where the value of E_g obtained from solution absorption spectra according to published method[4, 5], LUMO = lowest unoccupied molecular orbital = E_g+ HOMO.

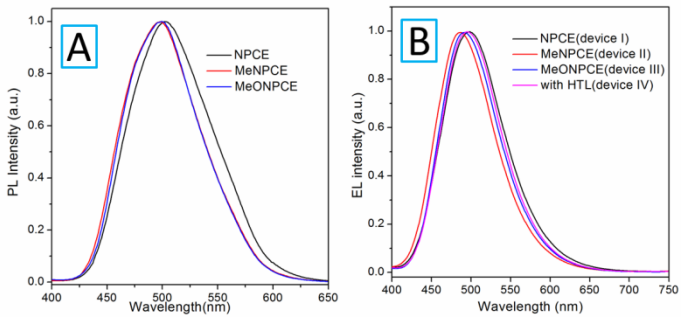

Fig. S16 (A) Amorphous PL spectra and (B) EL spectra of NPCE, MeNPCE and MeONPCE.

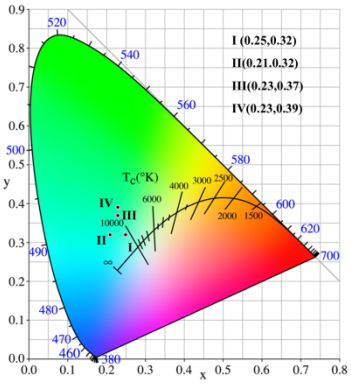

Fig. S17 CIE coordinates of the all OLED devices.

References

1. Y. Feng, Q. R. Chen, W. S. Li and C. Xie, Chem Res Appl, 2007, 19, 1162-1165.
2. R. Hu, J. L. Maldonado, M. Rodriguez, C. Deng, C. K. W. Jim, J. W. Y. Lam, M. M. F. Yuen, G. R. Ortiz and B. Z. Tang, J Mater Chem, 2012, 22, 232-240.
3. X. F. Duan, J. Zeng, Z. B. Zhang and G. F. Zi, J Org Chem, 2007, 72, 10283-10286.
4. E. W. R. Cristiano, I. H. Bechtold, A. J. Bortoluzzi and H. Gallardo, Tetrahedron, 2007, 63, 2851-2858.
5. H. Zhao, Y. Wang, Z. Liu and B. Dai, RSC Adv, 2014, 4, 13161-13166.